ALTERNATIVE GRAVIMETRIC METHODOLOGY FOR ISOSTATIC ANALYSES. AN EXAMPLE FOR BOLIVIAN ANDES

Carolina B. CROVETTO & Antonio INTROCASO

Abstract.- In this work we present a new, alternative methodology for performing isostatic studies by means of geoid undulations, excluding the use of measured gravity anomalies. An example on Bolivian Andes is presented as case study. Considering a digital elevation model as input data, a theoretical perfectly isostatically balanced Airy crustal model was constructed for Bolivia. The free-air and the Bouguer anomalies, and the geoid undulations produced by this theoretical model, were directly evaluated by means of three-dimensional integration. The "real" geoid undulations were computed from the EGM96 global geopotential model, and were filtered from long wavelengths by means of a sparse Fourier transform method. The residual "real" geoid undulations were compared with the theoretical geoid undulations for Bolivian Andes, showing a global tendency towards isostatic balance, agreeing with previous results obtained using traditional gravimetry.

The free-air and the Bouguer anomalies from the EGM96 residual geoid undulations were also evaluated and then compared with the anomalies produced by the theoretical model. The Bouguer anomalies support definitely the results obtained using the geoid undulations while the free-air anomalies, although less consistently, showed the same global tendency.

Key-words: Geoid; Gravity anomalies; Isostasy; New methodology; Bolivian Andes.

Resumen.- *Método gravimétrico alternativo para análisis isostáticos. Ejemplo sobre los Andes Bolivianos.* En este trabajo presentamos una nueva metodología alternativa para realizar estudios isostáticos empleando ondulaciones del geoide, sin utilizar anomalías de gravedad observadas. Un ejemplo sobre los Andes Bolivianos se presenta como caso de estudio. Considerando un modelo digital de elevación como dato de entrada, se construyó un modelo cortical teórico perfectamente balanceado siguiendo la hipótesis de Airy para Bolivia. Las anomalías de aire libre y de Bouguer, y las ondulaciones del geoide producidas por dicho modelo teórico se evaluaron directamente mediante integraciones en tres dimensiones. Las ondulaciones del geoide "reales" se obtuvieron a partir del modelo geopotencial global EGM96, de las cuales se filtraron las largas longitudes de onda mediante el empleo de una transformada de Fourier rala. Las ondulaciones del geoide "residuales" fueron comparadas con las ondulaciones teóricas en los Andes Bolivianos, mostrando una tendencia general al equilibrio isostático, en total acuerdo con los resultados gravimétricos previos.

Se evaluaron también las anomalías de aire libre y de Bouguer a partir de las ondulaciones del geoide residuales derivadas del EGM96, las cuales se compararon con las anomalías de gravedad generadas por el modelo teórico. Las anomalías de Bouguer certificaron definitivamente el resultado encontrado empleando el geoide, y las anomalías de aire libre, si bien resultaron menos consistentes, mostraron la misma tendencia global.

Palabras clave: Geoide; Anomalías de gravedad; Isostasia; Nueva metodología; Andes Bolivianos.

Carolina Beatriz Crovetto [e-mail: carolina@crovetto.com]: *Grupo de Geofísica, Instituto de Física Rosario, Av. Pellergini 250, Rosario, Argentina.*

Antonio Introcaso [e-mail: geofisic@fceia.unr.edu.ar]: *Grupo de Geofísica, Instituto de Física Rosario (CONICET – UNR), Av. Pellegrini 250, Rosario, Argentina.* [Correspondence author].

Bol. Inst. Fis. Geol. **78**: 1-12.
Rosario - Argentina.

Copia Impresa / Printed Copy [€ 12+5]
http://www.fceia.unr.edu.ar/fisiografia

INTRODUCTION

Isostasy studies the equilibrium of the crust and the lithosphere of the Earth. Isostatic balance is usually analysed employing isostatic anomalies, derived from measured gravity values. These anomalies are compared with those produced by a balanced model, assuming different isostatic hypothesis (Airy 1855, Pratt 1855, Vening Meinesz 1931).

In this work we propose a new alternative methodology to carry out the isostatic studies without using directly measured gravity values. We compare the real geoid undulations with the geoid undulations produced by a theoretical balanced model. The actual geoid undulations are extracted from a global geopotential model (EGM96 model) and the theoretical balanced model is constructed using a digital elevation model (GLOBE) from which Airy's roots are assumed (Heiskanen & Moritz 1967). Both data sources are freely-available, avoiding the necessity of field measurement. To perform further analyses the gravity anomalies are derived from the same global geopotential model EGM96 and compared with the gravity anomalies predicted by the same theoretical balanced model. Measured gravity anomalies are also employed for validation.

In order to test the new method, it is applied to the Bolivian Andes, which have been widely studied by different authors employing traditional gravimetry, and show a clear tendency to isostatic balance in Airy hypothesis (Lyon-Caen et al. 1985; Isacks 1988; Abriata & Introcaso 1990; Watts et al. 1995; Götze & Kirchner 1997; Lamb 2000; Introcaso et al. 2000a; Miranda & Introcaso 2000a; Götze & Krause 2002). Present study is preceded by two recent papers in which the geoid undulations along profiles were studied. Introcaso & Introcaso (2004) carried out a crustal analysis from geoid undulations along a profile in the Bolivian Andes at 22ºS, and Miranda & Introcaso (2000b) analyzed geoid values along an East-West section in the Bolivian Andes at 20ºS.

In spite of its application to Bolivian Andes, the methodology here presented is not restricted to high topographies. The authors and collaborators have also tested this methodology for the study of sedimentary basins (e.g., the Salado Basin, see Crovetto et al. 2007), with very promissory results.

METHODOLOGY

The traditional isostatic analysis involves the use of isostatic gravity anomalies. Following the notation of Heiskanen and Moritz (1967), isostatic anomalies are:

$$\Delta g_I = g_0 + F - A_B + A_t + A_C - \gamma \qquad \textbf{(Eq. 1)}$$

where g_0 is measured gravity, F is free-air correction, A_B is Bouguer correction, A_t is terrain correction, A_C is isostatic correction (which depends on the system considered), and γ is normal gravity in the comparison system (for example WGS84 ellipsoid). We need to know g_0 to calculate Δg_I; that is to say, we need gravimeters to indirectly obtain isostatic anomalies.

The gravity field can be defined in outer space using gravity vectors as well as equipotential surfaces, as the geoid or Earth's physical surface. Geoid can be calculated from: i) gravity anomalies using Stokes' formula or equivalent sources, ii) astrogeodetic deflections of the vertical or differences between ellipsoidal and orthometric heights *h-H*, iii) satellite orbits' deformations, gravity anomalies, deflections of the vertical and general data combination. Geoid undulations computed by technique ii), especially *h-H*, avoid the use of gravimeters. Through technique iii), global geopotential models are constructed.

We will use as input data a digital elevation model and geoid undulations. We will show that it is possible to analyse the isostatic state of a geological structure using these data.

From the digital elevation model can be constructed an isostatically balanced model. The free-air anomaly Δg_F for such model is:

$$\Delta g_F = g_t + g_c \qquad \textbf{(Eq. 2)}$$

where g_t represents the attraction of the topography (visible masses) and g_c is the attraction of the compensation root (hidden masses). g_c is negative because of the density contrast.

From Eq. 2, the Bouguer anomaly is:

$$\Delta g_B = g_c \qquad \textbf{(Eq. 3)}$$

We can also calculate the theoretical geoid undulations generated by our balanced model, through the computation of the gravity potentials produced by the topographic and the compensation masses. Applying the expression of Bruns (1878), $N = T/\gamma$, geoid undulations N are:

$$N = \frac{1}{\gamma}\left(T_t + T_c\right) \qquad \textbf{(Eq. 4)}$$

where γ is normal gravity (980 mGal), T_t is the topographic perturbing potential and T_c is the compensation root perturbing potential. We adopt the anomalies given by Eq. 2 and Eq. 3, and geoid undulations from Eq. 4 derived from this perfectly balanced model as comparison values.

On the other hand the free-air and Bouguer anomalies can be derived from the actual geoid undulations N' (real expression of the studied zone). Different methods can be applied to obtain the free-air anomaly $\Delta g'_F$ (for example: the planar formula of Stokes, equivalent sources or numerical vertical derivation).

From the free-air anomaly $\Delta g'_F$ and the digital elevation model, we can compute the Bouguer anomaly $\Delta g'_B$:

$$\Delta g'_B = \Delta g'_F - A_B \qquad \textbf{(Eq. 5)}$$

where $A_B = 2\pi G H \rho_t$ is the classical correction of Bouguer (ρ_t is the topographic density, G is the gravitational constant and H is the altitude). Comparing $\Delta g'_F$ and $\Delta g'_B$ anomalies and the "real" geoid undulations N' with those derived from our balanced model [Δg_F (Eq. 2), Δg_B (Eq. 3), N (Eq. 4)], the isostatic state and the crustal thickness of the studied area can be evaluated.

This methodology is applied to the study of the Bolivian Andes in the present paper. In the following, several planar approximations are used without taking into account the curvature of the Earth. In addition, the data used (digital elevation model, global geopotential model
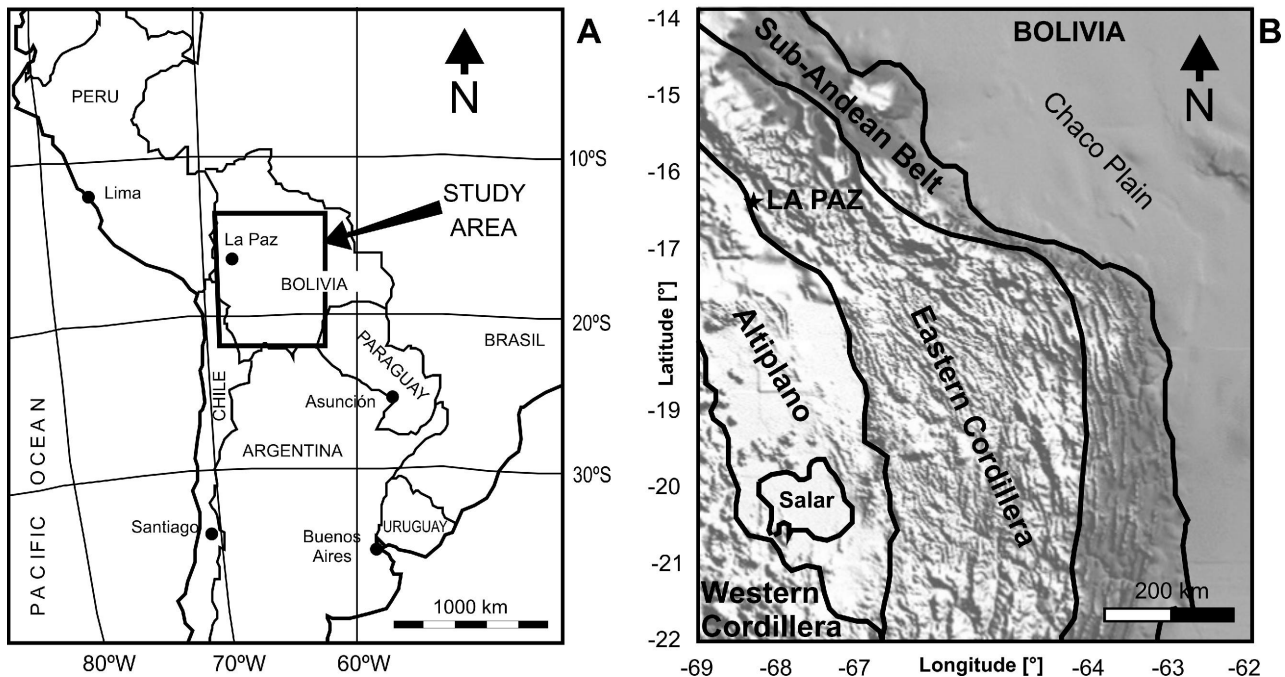
Figure 1. A: Location of the studied area in Bolivia. **B:** Tectonomorphic units of the Andean chain.

for Bolivia and gravity charts) could be not enough accurate to allow the construction of reliable charts. Nevertheless, we consider that the obtained results permit to carry out the regional isostatic analysis within an acceptable accuracy.

STUDY AREA

The study area is located in Bolivia and extends between 14° and 22° South latitude, and 69° and 62° West longitude (Fig. 1A). It comprises the Andean orogen and part of the Chaco Plain (Fig. 1B). The Central Bolivian Andes reach altitudes of 6000 m; the deformation zone extends from the Pacific trench axis to approximately 1000 km into the continent. The Bolivian Andes are divided into parallel tectonomorphic units (Fig. 1B); from west to east: 1) the Western Cordillera is the actual volcanic arc with mountains which locally reach 6000 m altitude; 2) the Altiplano is a high plateau with 3800 m average elevation; 3) the Eastern Cordillera, with mountains reaching 5000 m; 4) the Sub-Andean belt, with mean altitudes of 1500 m and 5) the Chaco Plain. A more detailed description of the tectonomorphic units can be found in Kennan et al. (1995).

Previous geophysical studies (Lyon-Caen et al. 1985; Abriata & Introcaso 1990; Watts et al. 1995; Götze & Kirchner 1997; Miranda & Introcaso 2000a; Götze & Krause 2002) reveal that the Western Cordillera, the Altiplano and the Eastern Cordillera are in isostatic balance considering Airy system, while the Sub-Andes and the Chaco Plain respond to a flexural system. This fact has been interpreted as the result of the flexure of the Brazilian Shield under the load of the Sub-Andes and part of the Eastern Cordillera (Lyon-Caen et al. 1985; Watts et al. 1995; Tassara 2005). Since the aim of the present study is to evaluate the use of geoid undulations to make isostatic studies but not to make a detailed model of the study area,

we have considered local equilibrium for the whole area to simplify the theoretical model and to test the proposed methodology.

THEORETICAL ISOSTATIC MODEL

As indicated above the digital elevation model GLOBE (GLOBE Task Team 1999) is used as input signal. Topographic contours for the study area are shown in Fig. 2A. GLOBE is an internationally developed and independently peer-reviewed global digital elevation model (DEM) with 30 arc-seconds latitude-longitude grid spacing. Horizontal precision is in general less than 1 km and vertical precision for South America has a mean square error of 152 m (Hastings & Dunbar 1999). Considering an average elevation of about 3-3.5 km for the studied area, this precision leads to mean altitude errors of about 4-5%. The uncertainty in the computation of the geoid undulations introduced by this error can be easily estimated by employing the one-dimensional approximation from Turcotte & Schubert (1982) as developed below. The uncertainty of 152 m in the topography of an isostatically balanced structure of 3 km mean elevation, introduces an uncertainty of 1 m in the geoid undulations produced by such structure. Considering that the approximation developed by Turcotte & Schubert (1982) over-estimates the geoid undulations in about 10-20% for structures like the one studied here (Crovetto et al. 2006), the average error in the geoid undulations introduced by the error in the digital elevation model is about 0.8-0.9 m, which represents less than 10% of the total undulation, and is considered appropriate for a regional isostatic study.

We assume perfect Airy isostatic balance (Airy 1855) and consider a topographic density $\rho_t = 2.67$ g cm^{-3}, a normal crustal thickness $T_N = 33$ km, and a density
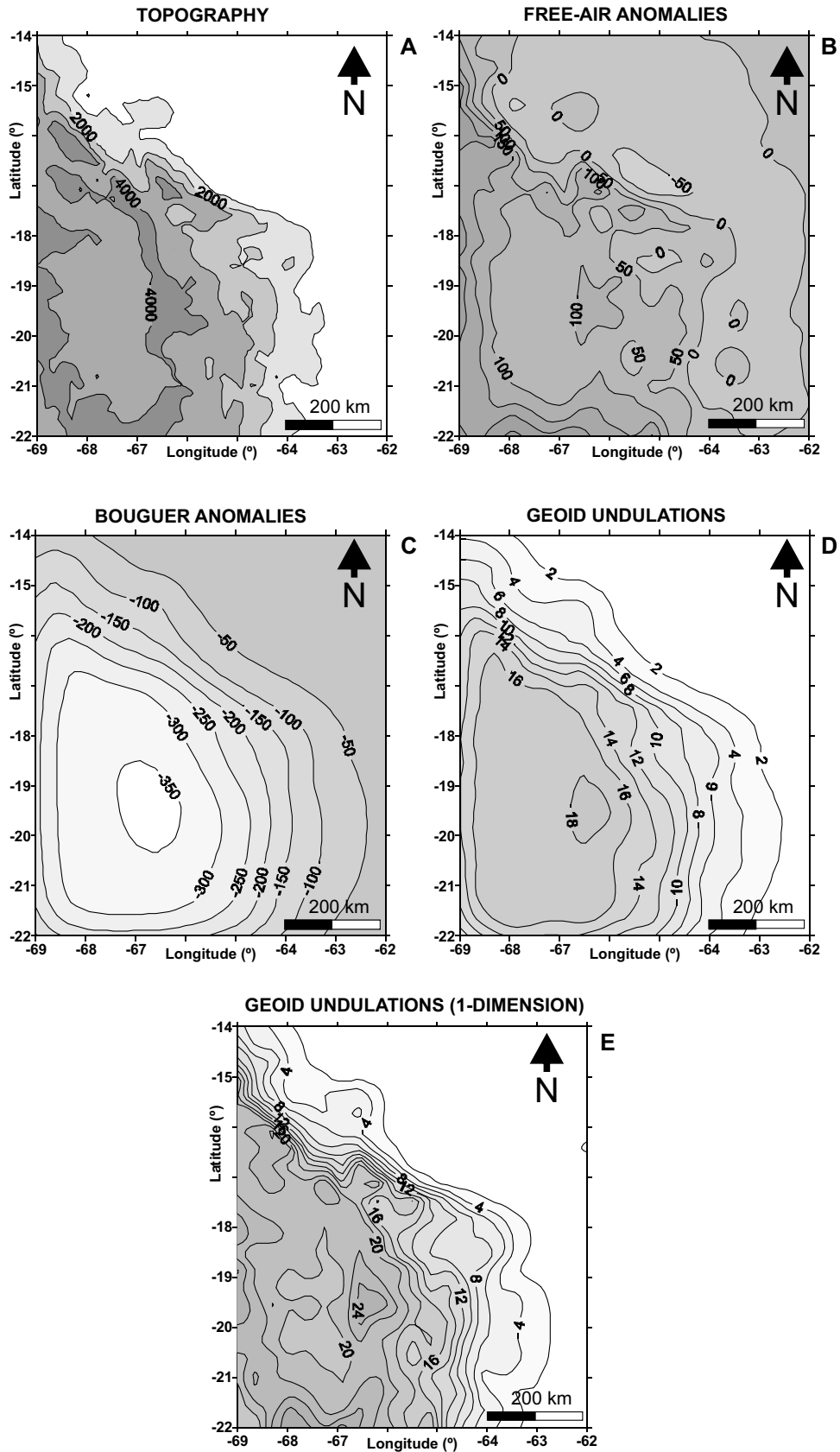
Figure 2. A: Topographic contours for Bolivia from GLOBE digital elevation model (contour interval 1000 m). **B:** free-air anomalies (g_F, contour interval 50 mGal). **C:** Bouguer anomalies (g_B, contour interval 50 mGal). **D:** geoid undulations (*N*, contour interval 2 m) calculated from our isostatic balanced model. **E:** One-dimensional geoid undulations computed from topography using the planar expression from Turcotte & Schubert (1982) (*N*, contour interval 2 m).
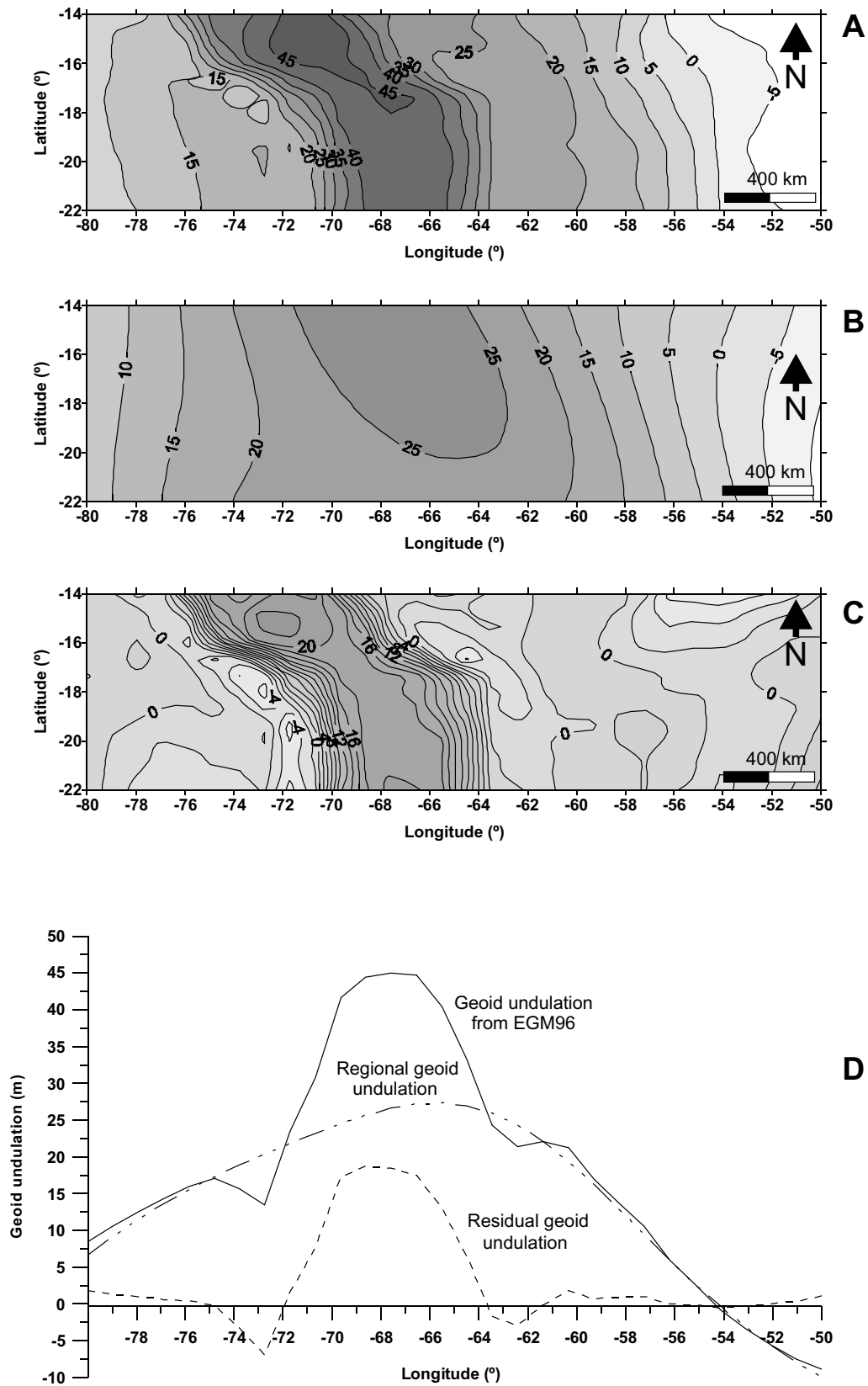
Figure 3. A: Geoid undulations derived from EGM96 geopotential model (contour interval 5 m). **B:** Regional geoid undulations obtained applying the sparse Fourier transform method to the undulations shown in Figure 3A (contour interval 5 m). **C:** Residual geoid undulations (contour interval 2 m). **D:** Profile along 18º S showing EGM96 (solid line), regional (dash and dot line) and residual (dashed line) geoid undulations.
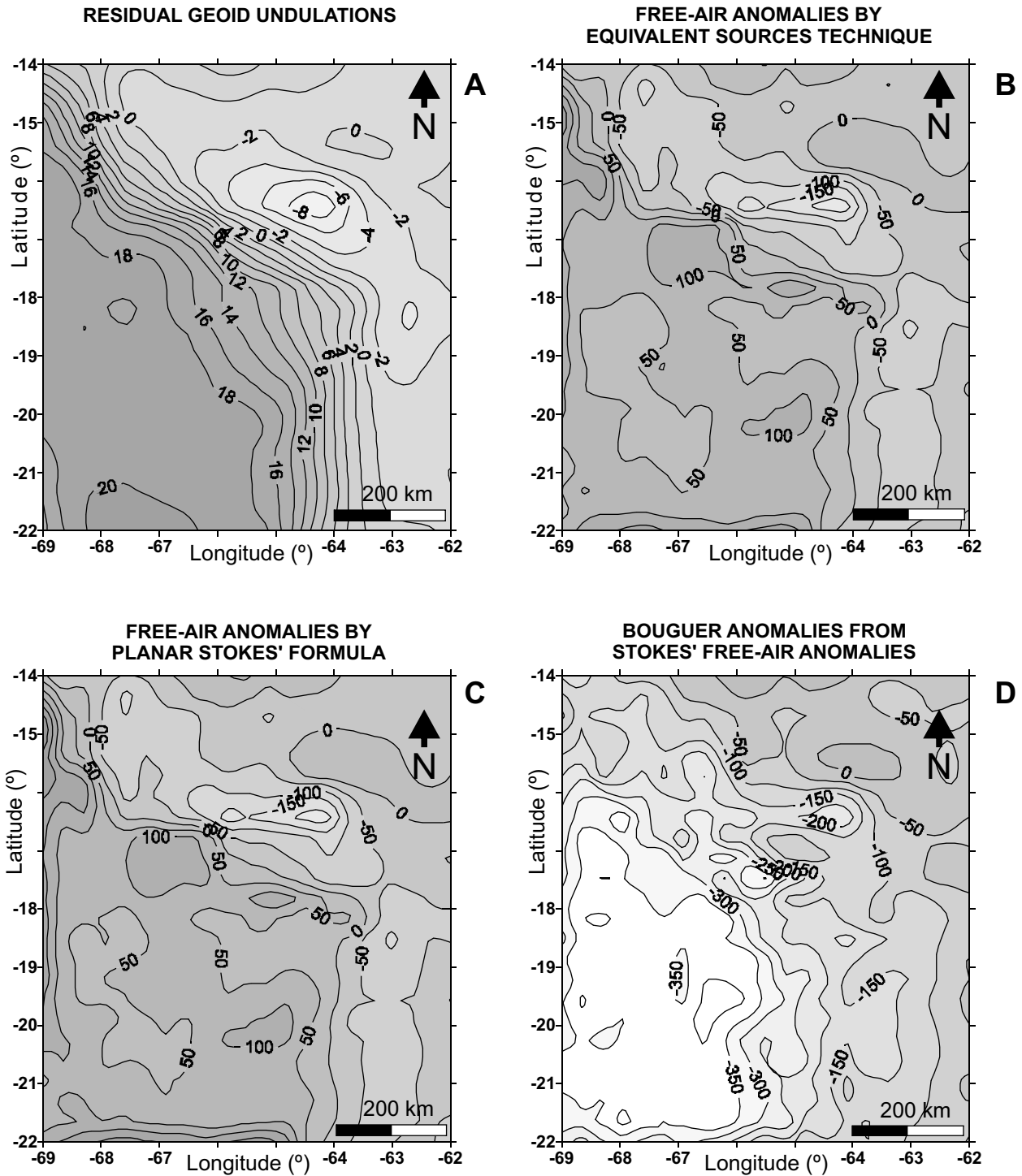
Figure 4. A: Residual geoid undulations for the studied area obtained through the sparse Fourier transform method (contour interval 2 m). **B:** Free-air anomalies obtained from the residual geoid undulations shown in Figure 4A using the equivalent sources technique (contour interval 50 mGal). **C:** Free-air anomalies obtained from the residual geoid undulations shown in Figure 4A with the planar formula of Stokes (contour interval 50 mGal). **D:** Bouguer anomalies derived from the free-air anomalies shown in Figure 4C, using the classical correction of Bouguer and considering the digital elevation model GLOBE (contour interval 50 mGal).

contrast between the lower crust and the upper mantle $=$ -0.4 g cm^{-3} (Introcaso et al. 2000b). Although the study area is large, planar approximations are used. Dipoles contribution to gravity and geoid undulations, produced by a balanced model, decay faster with distance than single-masses contribution because of the compensation between positive and negative masses. Using a simple model, we estimated that the geoid undulations produced by a massive dipole are negligible beyond 150 km. Within such area, differences between spherical formulae and planar approximations are smaller than 4% for close contributions (< 100 km), and smaller than 9% for distant

FREE-AIR ANOMALIES   **BOUGUER ANOMALIES**
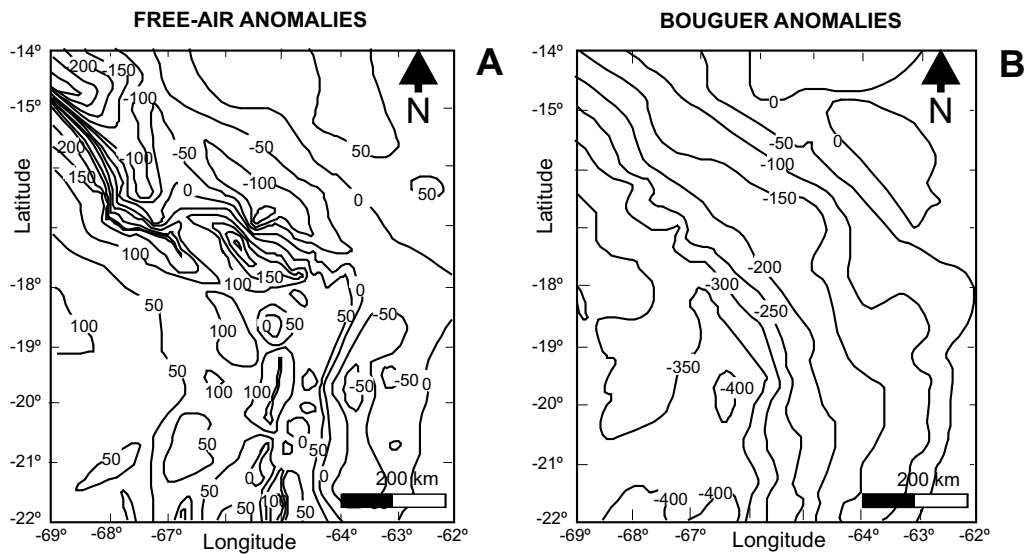

Figure 5. A: Observed free-air anomalies (contour interval 50 mGal). **B:** Observed Bouguer anomalies (contour interval 50 mGal). Source: Military Geographic Institute of Bolivia.

ones (< 150 km). Gravity attractions g_z (x,y,z) of topographic masses and buried compensation masses were computed dividing the corresponding structures in right parallelepipeds. The vertical attraction of a single parallelepiped can be analytically integrated (Introcaso & Huerta 1976; Nagy, 1966) as:

$$g_z(x,y,z) =$$

$$G.\rho \left\| \left| x \ln(y+r) + y \ln(x+r) + 2z \arctan \frac{x+y+r}{z} \right|_{\Delta x_1}^{\Delta x_2} \right|_{\Delta y_1}^{\Delta y_2} \Big|_{\Delta z_1}^{\Delta z_2}$$

(Eq. 6)

where is the density of the parallelepiped, (x, y, z) are the coordinates of the computation point, $x_1, x_2, y_1, y_2, z_1, z_2$ are the coordinates of the vertices of the parallelepiped and $r = [(x_i)^2 + (y_i)^2 + (z_i)^2]^{1/2}$ is the distance between the computation point and the parallelepiped vertices with $x_i = x-x_i$, $y_i = y-y_i$, $z_i = z-z_i$, $i = 1, 2$.

Free-air anomalies were calculated adding the attractions of the topographic and compensation masses with their signs using Eq. 2, while buried (i.e. compensation) masses' attractions (placed below the geoid height) were directly interpreted as Bouguer anomalies (Eq. 3). Topographic and compensation masses' gravity potentials $T(x,y,z)$ were also computed dividing the corresponding structures in right parallelepipeds. Using the same notation as in Eq. 6, the potential of a single parallelepiped becomes (Guspí 1999):

$$T(x,y,z) =$$

$$G.\rho \left\| \left| xy \ln(z+r) + xz \ln(y+r) + yz \ln(x+r) + x^2 \arctan \frac{y+z+r}{x} + \right. \right.$$

$$\left. + y^2 \arctan \frac{x+z+r}{y} + z^2 \arctan \frac{x+y+r}{z} \right|_{\Delta x_1}^{\Delta x_2} \Big|_{\Delta y_1}^{\Delta y_2} \Big|_{\Delta z_1}^{\Delta z_2}$$

(Eq. 7)

From the anomalous total potential T generated by the topographic and compensation structures, geoid undulations were calculated using the expression $N = T/$ (Bruns 1878).

Fig. 2A shows the topography (input data) while Fig. 2B-D show the gravity anomalies and the geoid undulations computed for our predictive isostatically balanced model. There is good correlation between the topography and the free-air anomalies, the Bouguer anomalies and the geoid undulations.

In order to evaluate the accuracy of the geoid undulations obtained (Fig. 2D), we also derived them from the digital elevation model, applying the one-dimensional planar formula proposed by Turcotte & Schubert (1982) for continental zones. This expression involves only the topography as input signal, obtaining the geoid undulations through an approximation similar to the slab concept of Bouguer. The geoid undulation produced by an isostatically balanced topography considering this one-dimensional approximation is:

$$N = \frac{\pi G}{\gamma} \rho_{uc} \left[2T_N H + \frac{\rho_{um} + \rho_{uc} - \rho_{lc}}{\rho_{um} - \rho_{lc}} H^2 \right]$$ **(Eq. 8)**

where $_{uc}$ is upper crust density, $_{lc}$ is lower crust density, $_{um}$ is upper mantle density, T_N is normal crustal thickness, and H is orthometric height.

The geoid undulations computed using Eq. 8 (Fig. 2E) are in average 10% higher than those calculated previously (Fig. 2D). Such difference can be attributed to the over-estimation of the structure's mass because of its replacement by an infinite slab, and it is consistent with predicted differences found for one-dimensional approximations (Crovetto et al. 2006). The geoid undulations so obtained validate the geoid undulations obtained by the parallelepiped technique, and show the limitations of these widely employed one-dimensional approximations (Crovetto et al. 2006).
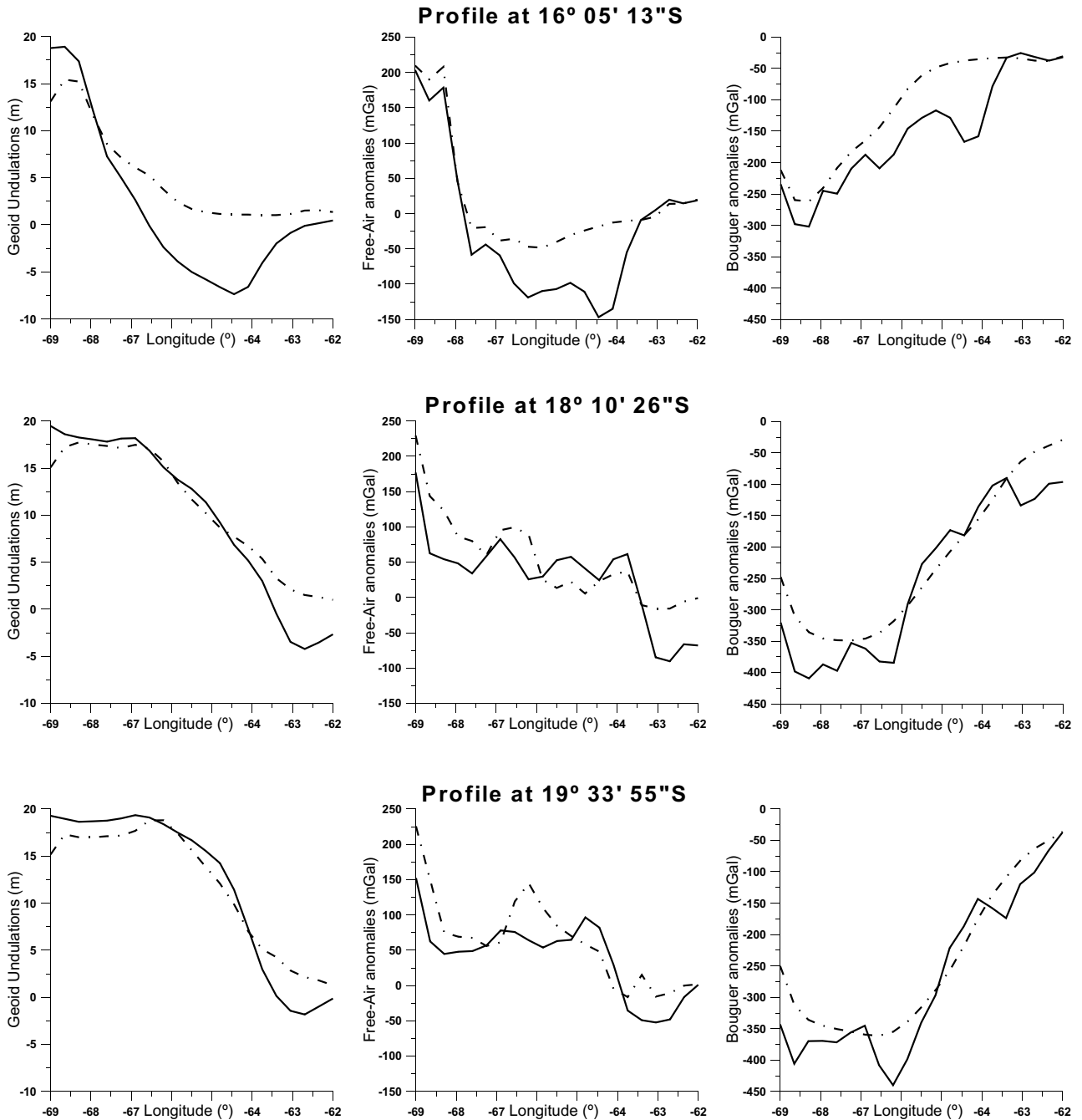
Profile at 16° 05' 13"S

Profile at 18° 10' 26"S

Profile at 19° 33' 55"S

Figure 6. Geoid undulations, free-air and Bouguer anomalies showing observed real values (solid line) and theoretical values (dash and dot line) along profiles at 16°, 18° and 19.5° S approximately.

"REAL" GEOID UNDULATIONS

"Real" geoid undulations were derived from the global geopotential model EGM96 (Lemoine et al. 1998). The poor resolution of this model, with errors of ±1 m in continents (Sideris 1996), introduces an error smaller than 10% in the geoid undulations within our study area. This error, which is compatible with the error of the digital elevation model, is acceptable for a regional isostatic study, and thus we considered the EGM96 model as appropriated for this study.

EGM96 geoid model considers the whole planet masses, involving different wavelengths which must be separated to identify the local effect of the orogen studied here. For discriminating the different components and isolating the Andean effect, EGM96 geoid undulations were calculated for a broader zone including the studied area. The geoid anomaly caused by the Andes can be clearly identified (Fig. 3A). The existence of such anomaly has already been pointed out by Froideveaux & Isacks (1984) and by Introcaso et al. (2000a). For filtering geoid undulations we applied a sparse Fourier transform method (Guspí & Introcaso 2000), which is based on the estimation of a high resolution discrete Fourier transform (DFT). The

incorporation of a priori information allows obtaining a sparse estimate of the DFT, thus the potential field can be defined through a combination of few simple functions. At the same time, low and high frequency components are easily distinguished, allowing us to isolate low frequencies and obtain long wavelengths, which correspond to the regional geoid (Fig. 3B).

The residual geoid undulations (Fig. 3C) were obtained by removing the regional undulations (Fig. 3B) from EGM96 (Fig. 3A). Fig. 3D shows the corresponding total, regional and residual geoid undulations in a profile along 18°S. There is an important similitude between our Fig. 3D and the fig. 3 in Froideveaux & Isacks (1984), where geoid undulations along a section at 20ºS were studied. Fig. 4A shows a more detailed residual geoid undulations map for the studied area.

GRAVITY ANOMALIES FROM RESIDUAL GEOID UNDULATIONS

Using the residual "real" geoid undulations obtained above as input data (Fig. 4A), two different methods were applied to compute the "real" free-air anomaly (Introcaso et al. 2007). In a first approach, the equivalent sources technique was used (Cordell 1992; Guspí et al. 2004). Once the anomalous potential was derived from the residual geoid undulations through the expression of Bruns (1878), a set of punctual masses is obtained, which reproduces the potential field. Then, the gravity attraction corresponding to such masses is computed, and directly interpreted as free-air anomalies (Fig. 4B). In a second approach it was applied the planar formula of Stokes (1849). For obtaining the geoid undulations corresponding to a plain surface, the integral of Stokes (1849) yields:

$$N(x,y) =$$
$$\frac{1}{2\pi\gamma} \int_{-\infty}^{\infty} \int_{-\infty}^{\infty} \Delta g_F(x',y',0) \left[(x-x')^2 + (y-y')^2 \right]^{-\frac{1}{2}} dx'dy'$$

(Eq. 9)

where $N(x,y)$ represents the undulation at any point $P(x,y)$ and $g_F(x'y',0)$ is the free-air anomaly at other point on the geoid. If we assume Helmert condensation method (Heiskanen & Moritz 1967), the indirect effect produced by a topography with a height of 3 km can be easily estimated (Rapp & Wichiencharoen 1984) yielding 0.52 m, while its direct effect on gravity anomalies is 3 mGal. This change from co-geoid to geoid is negligible for our purposes (it represents less than 5 % of total undulation), so we have not considered further corrections. Eq. 9 can be solved dividing the integration surface in rectangular cells, and considering constant gravity within each cell (Introcaso & Crovetto 2005):

$$N(x,y) = \frac{1}{2\pi\gamma} \sum_i \sum_j \Delta g_F(x_i, y_j, 0) \cdot F^{ij}(x,y)$$

(Eq. 10)

The function $F^{ij}(x,y) = \iint_{ij-cell} \left[(x-x')^2 + (y-y')^2 \right]^{-\frac{1}{2}} dx'dy'$ can be integrated analytically (Chapman 1979) and is proportional to the gravity potential produced by the *ij*-cell at the point $P(x,y)$; $g_F(x_i y_j, 0)$ is the free-air anomaly at the

central point of the *ij*-cell. Considering Eq. 10 as a linear system of equations, free-air anomalies can be obtained from geoid undulations. This free-air anomalies chart (Fig. 4C) show very good correlation with that obtained previously (equivalent sources technique, Fig. 4B), validating our results. From the free-air anomalies (Fig. 4C), the Bouguer anomalies (Fig. 4D) were calculated using the classical correction of Bouguer (Eq. 5), considering a topographic density $_t$ = 2.67 g cm^{-3} and the digital elevation model GLOBE.

MEASURED GRAVITY ANOMALIES

Free-air and Bouguer anomalies charts (Fig. 5), constructed by the Military Geographic Institute of Bolivia in cooperation with the Geophysical Institute of Bolivia (Instituto Geográfico Militar Boliviano 1971, 1972) were also employed. Although these charts are not up to date, they were used for validating the anomalies derived from the global geopotential model EGM96.

DISCUSSION

For the analysis of the isostatic behaviour of the Bolivian Andes, theoretical and "real" geoid undulations and anomalies were compared.

We computed the geoid undulations corresponding to a perfectly balanced isostatic model considering the system of Airy. To calculate such undulations, we used two different techniques: the decomposition of the structure in right parallelepipeds (Fig. 2D) and the planar expression from Turcotte & Schubert (1982), see Fig. 2E. The expression of Turcotte & Schubert (1982) is just an approximation to the real undulations caused by balanced structures, and over-estimates geoid undulations values. The parallelepiped technique is more accurate and also involves x and y dimensions. In the following analyses, we considered the results obtained applying this last technique.

The residual "real" geoid undulations (Fig. 4A) show qualitative and quantitative correlation with the theoretical geoid undulations (Fig. 2D). The determination coefficient (Hildebrand & Lyman 1997) between "real" and theoretical undulations is 0.76. The main difference between both maps is a negative undulations' zone in the "real" geoid undulations (Fig. 4A), which does not exist in the theoretical ones (Fig. 2D). This zone, located at 16ºS, 64ºW, would correspond to an anomalous zone having no relation with the topography. If we do not consider this anomalous area, the determination's coefficient rises to 0.77. We can also compare "real" and theoretical geoid undulations along the profiles shown in Fig. 6. Along the first profile (16º 05' 13" S), there is poor correlation. This fact could be explained considering that this profile crosses the above mentioned anomalous area. Along the two other profiles (18º 10' 26"S and 19º 33' 55"S) there is very good correlation. The comparison between "real" and theoretical geoid undulations suggests that the Bolivian Andes would show a tendency to isostatic balance in Airy system.

"Real" (Fig. 2B) and theoretical (Fig. 4B and Fig. 4C) free-air anomalies maps show poor correlation. A large area with anomalous values (50-100 mGal) and a well-defined line of 0 mGal crossing the zone from NW to

SE can be seen in both maps. Again, there is an anomalous zone with negative free-air anomalies located at 16ºS, 64ºW. Within that zone, "real" negative anomalies are higher in absolute values (-200 mGal) than those predicted by the theoretical model (-50 mGal), a behaviour uncorrelated with topography. The determination coefficient between the "real" and theoretical free-air anomalies is 0.6 (without considering the anomalous area), indicating poor correlation. The comparison along the profiles in Fig. 6 confirms this behaviour, with a very poor correlation between "real" and theoretical free-air anomalies in the first profile (that which crosses the anomalous area), and a moderate correlation in the other two profiles. This poor correlation between "real" and theoretical free-air anomalies may be attributed to the important oscillation of these anomalies, due to the significant influence of topography (Fig. 2A). This oscillation is not present in Bouguer anomalies, which are more regular (Woollard 1969). The Bouguer anomalies corresponding to the balanced model (Fig. 2C) agree with those derived from EGM96 model (Fig. 4D); both of them show maximum amplitudes of -350 mGal and similar morphology. The "real" Bouguer anomalies present a local minimum (-200 mGal) in the mentioned anomalous area of negative free-air anomalies and geoid undulations located at 16ºS, 64ºW. The determination coefficient between the "real" and the theoretical Bouguer anomalies is 0.84, considering the anomalous area. The comparison between "real" and theoretical Bouguer anomalies along the profiles in Fig. 6 confirms the good correlation.

The anomalous behaviour of "real" free-air and Bouguer anomalies and geoid undulations within the area placed at 16ºS, 64ºW, would suggest that some local isostatic unbalance could exist. The anomalous values found (negative free-air anomalies, negative geoid undulations and negative Bouguer anomalies) deserve further local studies.

Finally we observe that the measured gravity anomalies obtained by the Military Geographic Institute of Bolivia (Fig. 5) are similar to the "real" anomalies derived from the global geopotential model EGM96 (Fig.s 4C-D). This similitude supports the filtering procedure applied to geoid undulations and the methods applied to the computation of gravity anomalies from geoid undulations.

CONCLUSIONS

Crustal and isostatic studies are usually carried out through the comparison of observed gravity anomalies (calculated from gravity values determined by means of gravimeters) with those derived from theoretical isostatically balanced models. Thus, measured gravity values are indispensable for conducting these studies.
Different global geopotential models exist today, which are constructed combining satellite and terrain data. For example, the EGM96 model employed here (Lemoine et al. 1998), and some recently appeared models like the EIGEN-CG01C (Reigber et al. 2004) and the EIGEN-CG03C (Förste et al. 2005). In this work we have shown that comparing the geoid undulations from these global geopotential models with the geoid undulations computed for a perfectly isostatically balanced model, it is possible to carry out isostatic studies without the use of measured gravity values. The results of such comparison could be validated by employing for example *h-H* geoid

undulations values, which are independent of the global geopotential models. From these global geopotential models, it is also possible to derive the free-air and Bouguer gravity anomalies. The comparison between such anomalies and those calculated for the perfectly isostatically balanced model allows an alternative comparison to be done.

The new methodology proposed in this paper was employed to make an isostatic analysis of Bolivia as case study. Results suggests that Bolivian Andes are in local isostatic balance (Airy 1855), with the exception of an anomalous zone located at 16ºS, 64ºW in the Chaco Plain. These results are in very good agreement with previous studies conducted with traditional gravimetry for that area (Lyon-Caen et al. 1985; Isacks 1988; Abriata & Introcaso 1990; Watts et al. 1995; Götze & Kirchner 1997; Miranda & Introcaso 2000a; Götze & Krause 2002), showing the good performance of the new methodology.

REFERENCES

Abriata J.C. & Introcaso, A., 1990. Contribución gravimétrica al estudio de la transecta ubicada al sur de Bolivia. *Revista del Instituto Geográfico Militar, Año 5,* **7**: 8-19.

Airy G.B., 1855. On the computation of the effect of the attraction of mountain-masses, as disturbing the apparent astronomical latitude of stations of geodetic surveys. *Philosophical Transactions of the Royal Society of London* **145:** 101-104.

Bruns H., 1878. Die Figur der Erde. *Publikation Königl Preuss. Geodetic Institut Stankiewicz Buchdrukerei,* 98 p. Berlin.

Chapman M. E., 1979. Techniques for interpretation of geoid anomalies. *Journal of Geophysical Research* **84 (B8)**: 3793-3801.

Cordell L., 1992. A scattered equivalent-source method for interpolation and gridding of potential-field data in three dimensions. *Geophysics* **57(4)**: 629-636.

Crovetto C., Molinari R. & Introcaso A., 2006. Aproximaciones para el cálculo del geoide isostático. *Revista de la Asociación Geológica Argentina* **61(3)**: 38-48.

Crovetto C.B., Novara I.L. & Introcaso A., 2007. A stretching model to explain the Salado Basin (Argentina). *Boletín del Instituto de Fisiografía y Geología* **77(1-2):** 1-10.

Förste C., Flechtner F., Schmidt R., Meyer U., Stubenvoll R., Barthelmes F., König R., Neumayer K.H., Rothacher M., Reigber Ch., Biancale R., Bruinsma S., Lemoine J.-M. & Raimondo J.C., 2005. A new high resolution global gravity field model derived from combination of GRACE and CHAMP missions and altimetry/gravimetry surface gravity data. *EGU General Assembly 2005, Vienna, Austria*: 24-29. http://www.gfz-potsdam.de/pb1/op/grace/results/index_RESULTS.html.

Froideveaux C. & Isacks B., 1984. The mechanical state of the lithosphere in the Altiplano-Puna segment of the

Andes. *Earth & Planetary Science Letters* **71**: 305-314.

GLOBE Task Team and others (Hastings D., Dunbar P., Elphingstone G., Bootz M., Murakami H., Maruyama H., Masaharu H., Holland P., Payne J., Bryant N., Logan T., Muller J., Schreier G. & MacDonald J.), 1999. The Global Land One-kilometer Base Elevation (GLOBE) Digital Elevation Model, Version 1.0. *National Oceanic and Atmospheric Administration, National Geophysical Data Center, 325 Broadway, Boulder, Colorado 80303, U.S.A.* Digital data base at http://www.ngdc.noaa.gov/mgg/topo/globe.html.

Götze H.-J. & Kirchner A., 1997. Interpretation of gravity and geoid in the Central Andes between 20º and 29ºS. *Journal of South American Earth Sciences* **10(2)**: 179-188.

Götze H.-J. & Krause S., 2002. The Central Andean gravity high, a relic of an old subduction complex?. *Journal of South American Earth Sciences* **14**: 799-811.

Guspí F., 1999. Fórmulas compactas para el cálculo del potencial gravitatorio de prismas rectangulares. En: *Contribuciones a la Geodesia en la Argentina de fines del siglo XX – Homenaje a Oscar Parachú. UNR Editora:* 129-133.

Guspí F. & Introcaso B., 2000. A sparse spectrum technique for gridding and separating potential field anomalies. *Geophysics* **65(4)**: 1154-1161.

Guspí F., Introcaso A. & Introcaso B., 2004. Gravity-enhanced representation of measured geoid undulations using equivalent sources. *Geophysical Journal International* **158**: 1-8.

Hastings D. & Dunbar P., 1999. Global Land One-kilometer Base Elevation (GLOBE) Digital Elevation Model. *Documentation, Volume 1.0. Key to Geophysical Records Documentation (KGRD) 34. National Oceanic and Atmospheric Administration, National Geophysical Data Center, Boulder, Colorado.* http://www.ngdc.noaa.gov/mgg/topo/globe.html.

Heiskanen W. & Moritz H., 1967. Physical Geodesy. *W. Freeman and Company*, 364 pp., San Francisco.

Hildebrand D. & Lyman Ott R., 1997. Estadística aplicada a la administración y a la economía. *Addison Wesley Longman*, 943 pp.

Introcaso A. & Huerta E., 1976. Valuación de efectos gravimétricos y sus aplicaciones a la interpretación. *Geoacta* **8(1)**: 75-98.

Introcaso A., Cornaglia L. & Pacino M.C., 2000a Gravimetría en los segmentos andinos en 23ºS y 35ºS. Acortamientos, estado isostático y modelos corticales. *Actas del 22° Simposio sobre Latinoamérica, Stuttgart, Alemania* **18**: 49.

Introcaso A., Pacino M.C. & Guspí F., 2000. The Andes of Argentina and Chile: Crustal configuration, isostasy, shortening and tectonic features from gravity data. *Temas de Geociencia* **5**: 1-31.

Introcaso A. & Introcaso B., 2004. Estudio cortical en una sección de los Andes Bolivianos a partir de ondulaciones del geoide. *16 Congreso Geológico Boliviano, Oruro, Bolivia, 4 pp.* **[MSD 2]**

Introcaso A. & Crovetto C., 2005. Introducción a la construcción del geoide. *Temas de Geociencia* **12**: 1-56.

Introcaso A., Crovetto C.B., Introcaso B. & Ruiz F., 2007. Construction of gravity charts without observed gravity data. *Bolletino di geodesia e scienze affini*

66(4): 189-209.

Instituto Geográfico Militar Boliviano (en cooperación con el Instituto Geofísico Boliviano), 1971. Carta de anomalías de Bouguer de Bolivia. Escala 1:2.500.000.

Instituto Geográfico Militar Boliviano (en cooperación con el Instituto Geofísico Boliviano), 1972. Carta de anomalías de aire libre de Bolivia. Escala 1:2.500.000.

Isacks B., 1988. Uplift of the Central Andes plateau and bending of the Bolivian orocline. *Journal of Geophysical Research* **93**: 3211-3231.

Kennan L., Lamb S. & Rundle C., 1995. K-Ar dates from the Altiplano and Cordillera Oriental of Bolivia: implications for Cenozoic stratigraphy and tectonics. *Journal of South American Earth Sciences* **8(2)**: 163-186.

Lamb S., 2000. Active deformation in the Bolivian Andes, South America. *Journal of Geophysical Research*, **105(B11)**: 25627-25653.

Lemoine F., Kenyon S., Factor J., Trimmer R., Pavlis N., Chiuw D., Cox C., Klosko S., Lutheke S., Torrence M., Wang Y., Williamson R., Pavlis H., Rapp R. & Olson T., 1998. The development of the joint NASA, CSFC and NIMA geopotential model EGM96. *NASA/TP, Technical Report 1998 – 206861, Goddard Space Flight Center,* 575 pp. URL: http://cddis.nasa.gov/926/egm96/egm96.html.

Lyon-Caen H., Molnar P. & Suárez G., 1985. Gravity anomalies and flexure of the Brazilian Shield beneath the Bolivian Andes. *Earth and Planetary Science Letters* **75:** 81-92.

Miranda S. & Introcaso A., 2000a. Acortamientos corticales para los Andes Centrales Bolivianos a partir de datos de gravedad. *Actas del Noveno Congreso Geológico Chileno, Puerto Varas, Chile* **2**: 593-597.

Miranda S. & Introcaso A., 2000b. Anomalías de ondulación del geoide isostático para los Andes Centrales de Bolivia en 20ºS. Actas del *Vigésimo Congreso de la Asociación Argentina de Geofísicos y Geodestas, Mendoza, Argentina*: 207-211. **[MSD 1]**

Nagy D., 1966. The gravitational attraction of a right rectangular prism. *Geophysics* **31(2)**: 362-371.

Pratt J.H., 1855. On the attraction of the Himalaya mountains, and of the elevated regions beyond them, upon the plumb line in India. *Philosophical Transactions of the Royal Society of London* **14:** 53-100.

Rapp R. & Wichiencharoen C., 1984. A Comparison of Satellite Doppler and Gravimetric Geoid Undulations Considering Terrain-Corrected Gravity Data. *Journal of Geophysical Research* **89(B2)**: 1105-1111.

Reigber Ch., Schwintzer P., Stubenvoll R., Schmidt R., Flechtner F., Meyer U., König R., Neumayer H., Förste Ch., Barthelmes F., Zhu S.Y., Balmino G., Biancale R., Lemoine J.-M., Meixner H. & Raimondo J.C., 2004. A High Resolution Global Gravity Field Model Combining CHAMP and GRACE Satellite Mission and Surface Gravity Data: EIGEN-CG01C. URL: http://www.gfz-postdam.de/grace/results/index_results.html

Sideris M.,1996. International tests of the new GSFC/DMA Geopotential Models. Gravity, Geoid and Marine Geodesy. *International Association of Geodesy Symposia (Tokyo)* **117**: 478-485.

Stokes G.G., 1849. On the variation of gravity on the

surface of the earth. *Transactions of the Cambridge Philosophical Society* **8**: 672-695.

Tassara A., 2005. Interaction between the Nazca and South American plates and formation of the Altiplano-Puna plateau: Review of a flexural analysis along the Andes margin (15º-34ºS). *Tectonophysics* **399**: 39-57.

Turcotte D. L. & Schubert, G. 1982. Geodynamics. Applications of continuum physics to geological problems. *John Wiley & Sons Ed., New York*, 450 pp.

Vening Meinesz F.A., 1931. Une nouvelle méthode pour la réduction isostatique régionale de l'intensité de la pesanteur. *Bulletin Géodésique* **29**: 35-51.

Watts A.B., Lamb S.H., Fairhead J.D. & Dewey J.F., 1995. Lithospheric flexure and bending of the Central Andes. *Earth and Planetary Science Letters* **134**: 9-21.

Woollard G., 1969. Regional Variations in Gravity. *Geophysical Monograph, American Geophysical Union* **13**: 320-341.